

Thermodynamics and phase transitions in dissipative and active Morse chains

A.P. Chetverikov¹, W. Ebeling^{2,a}, and M.G. Velarde³

¹ Faculty of Nonlinear Processes, Saratov State University, Astrakhanskaya 83, 410012 Saratov, Russia

² Institut für Physik, Humboldt-Universität Berlin, Newtonstrasse 15, 12489 Berlin, Germany

³ Instituto Pluridisciplinar, Universidad Complutense, Paseo Juan XXIII, 1, 28040 Madrid, Spain

Received 10 August 2004 / Received in final form 27 January 2005

Published online 30 May 2005 – © EDP Sciences, Società Italiana di Fisica, Springer-Verlag 2005

Abstract. We study the evolution of a simple one-dimensional chain of $N = 4$ particles with Morse interactions and periodic boundary conditions which are imbedded into a heat bath creating dissipation and noise. The investigation is concentrated on thermodynamic properties for equilibrium, near-equilibrium and far-equilibrium conditions. For the thermodynamic equilibrium, created by white noise and passive friction obeying Einstein's fluctuation dissipation relation, we find a standard phase diagram. By applying active friction forces the system is driven to stationary non-equilibrium states, creating conditions where various self-sustained oscillations are excited. Thermodynamic quantities like energy, pressure and entropy are calculated near equilibrium, around a critical distance from equilibrium and far from equilibrium. We observe maximal order (minimum entropy) in certain region of the noise temperature, a phenomenon which is reminiscent of stochastic resonance. With increasing distance from equilibrium new "phases" corresponding to the existence of several attractors of the dynamical stem appear.

PACS. 05.40.-a Fluctuation phenomena, random processes, noise and Brownian motion – 05.70.Fh Phase transitions: general studies – 05.70.Ln Non-equilibrium and irreversible processes – 64.60.-i General studies of phase transitions

1 Introduction

We study here the thermodynamics and statistical physics of a driven – dissipative system. For simplicity we consider a one – dimensional lattice of four particles with periodic boundary conditions. The motivation for this work is the following: Phase transitions and critical phenomena are well understood at thermodynamic equilibrium. The corresponding phenomena occurring at non-equilibrium are only understood in the linear realm of irreversible phenomena. When we consider phenomena far from equilibrium the situation is quite different, as general thermodynamic framework is available. Thus we feel that a systematic exploration of simple model systems may be of help to provide the basis of a non-equilibrium thermodynamics and a theory of non-equilibrium transitions.

Following the pioneering work of Fermi, Pasta, and Ulam, and Toda [1], studies of one-dimensional nonlinear model systems have greatly contributed to our understanding of nonlinear excitations in various physical systems [2]. A topic of special interest is the coupling of finite size nonlinear ring chains to a heat bath and the properties of the resulting excitation spectra [3–7]. Progress has been

achieved in the numerical exploration of thermal excitations and clustering processes in one-dimensional Morse ring chains with small particle number N [8–10]. In particular, phase diagrams and collective excitations for the $N \leq 4$ case were determined. Here these investigations are extended to situations far from equilibrium. The case considered is that of a ring chain driven away from equilibrium by applying *active* friction forces. [6, 11–14]. In particular we show that several interesting nonlinear excitations as e.g. "dissipative" solitons may be excited. The concepts of "dissipative" forces and "dissipative" solitons were investigated recently both on the theoretical as well as on the experimental sides [16–19]. Another relevant concept, is that of active (nonlinear) Brownian motion [20–23]. The third important concept is connected with cluster formation. Clustering and Van der Waals type phase transitions are specific for systems with attractive interactions as e.g. Lennard-Jones and Morse potentials [8–10, 24].

The paper is organized as follows. In Sections 2 and 3 we introduce the equations of motion and recall earlier results needed here. Section 4 gives some analytical results for the thermodynamics of ideal systems. Section 5 contains a survey of the numerical algorithms and some results about the contributions of the interactions to the

^a e-mail: ebeling@physik.hu-berlin.de

thermodynamic functions. Section 6 deals with the total thermodynamic functions and a discussion of stochastic resonance and “phase transitions”. Since we are dealing here with small $1 - d$ systems we do not observe proper thermodynamic phase transitions but instead we see fast qualitative changes in a narrow region which are not connected with mathematical discontinuities of functions in the sense of Ehrenfest’s definitions.

2 Stochastic dynamics of Morse chains

We consider a one-dimensional model of N identical point-particles with masses m located on a ring of length L . This is equivalent to a linear system with periodic boundary conditions. The particles are described by coordinates $x_i(t)$ and velocities $v_i(t)$, $i = 1, \dots, N$ with

$$x_{i+N} = x_i + L. \quad (1)$$

The potential energy stored in the ring is

$$U = \sum_{i=1}^N U_i(r_i), \quad (2)$$

where $U_i(r_i) = U_i(x_{i+1} - x_i)$ denotes the Morse pair interaction potential explicitly given by

$$U_i(r_i) = \frac{a}{2b} [e^{-b(r_i-\sigma)} - 1]^2 - \frac{a}{2b} \quad (3)$$

with positive parameters $a, b, \sigma > 0$. We consider only nearest-neighbor (n.n.) interactions. The Morse potential has a minimum with the depth $\epsilon = a/2b$ at $r_i = \sigma$ and tends asymptotically to 0 for $r_i \rightarrow \infty$. The angular frequency of oscillations around the equilibrium distance is given by $m\omega_0^2 = ab$. The Morse potential (3) (akin to the Lennard-Jones potential) can also be considered as a generalization of Toda’s exponential potential [1]. In the limit of $r_i \ll \sigma$ the Morse potential is completely dominated by the exponential repulsive part. For Morse interactions σ gives the equilibrium length of the springs. Due to the coupling to the heat bath, the evolution is given by the Langevin equations

$$\begin{aligned} \frac{d}{dt}x_i &= v_i, \\ m\frac{d}{dt}v_i + \frac{\partial U}{\partial x_i} &= F(v_i) + m\sqrt{2D}\xi_i(t), \end{aligned} \quad (4)$$

governing the stochastic motion of the i th particle on the ring in the presence of dissipation and noise. The stochastic forces $\sqrt{2D}\xi_i(t)$ (Gaussian white noise), are characterized by

$$\langle \xi_i(t) \rangle = 0, \quad \langle \xi_i(t')\xi_j(t) \rangle = \delta_{ij}\delta(t' - t). \quad (5)$$

Following Lord Rayleigh we define the “dissipative” force as a velocity-dependent *active* friction function

$$F(v_i) = -m\gamma(v_i)v_i \quad (6)$$

consisting of an equilibrium and a non-equilibrium part

$$\gamma(v) = \gamma_0 + \gamma_1(v). \quad (7)$$

Here the first (constant) part γ_0 describes the standard friction between the particles and the surrounding heat bath. It obeys the Einstein relation [8, 23]

$$D = k_B T_b \gamma_0 / m. \quad (8)$$

where T_b is the (noise) temperature of the heat bath. Other temperature concepts will be discussed in the next section. The fluctuating force connected with the *passive* (equilibrium) friction γ_0 obeys the fluctuation-dissipation theorem (FDT) (8). The force corresponding to the *active* (non-equilibrium) friction, γ_1 , does not fluctuate in our model. A discussion of nonlinear systems, where the FDT differs from the simple Einstein relation (8), can be found in [20–22]. In accordance with earlier works [8, 13, 14, 23], we will model here the active part of the friction by the expression

$$\gamma_1 = -\gamma_0 \frac{\delta}{1 + v^2/v_d^2}. \quad (9)$$

Then the total friction force acting on a particle may be represented as

$$F(v) = -m\gamma_0 v \left[1 - \frac{\delta}{1 + v^2/v_d^2} \right]. \quad (10)$$

This friction force was introduced and investigated in [13, 14, 23] to model *active* Brownian particles that carry refillable energy reservoirs (internal degrees of freedom). In equation (10), the characteristic velocity $v_d > 0$ is connected to internal dissipation. The bifurcation parameter $\delta \leq 0$ controls the conversion of the energy taken up from the surrounding into kinetic energy. The value $\delta = 0$ corresponds to equilibrium, the region $0 < \delta < 1$ stands for nonlinear *passive* friction and $\delta > 1$ corresponds to *active* force. The bifurcation from one to the other regime occurs at $\delta = 1$. For the *passive* regime $0 < \delta < 1$ the friction force vanishes at $v = 0$ which is the attractor of the deterministic motion. Without noise all particles come to rest at $v = 0$. For $\delta > 1$ the point $v = 0$ becomes unstable but we have now two additional zeros at

$$v = \pm v_0 = v_d \sqrt{\delta - 1}. \quad (11)$$

These two velocities are the new attractors of the free deterministic motion if $\delta > 1$. In Figure 1 we have plotted the friction force for the two values $\delta = 0$ (equilibrium) and $\delta = 2$ (strong driving). The figure includes the representation of a useful piecewise linear approximation of the friction force for $\delta > 1$ which reads

$$F = -\gamma_{pl} v \left[1 - \frac{v_0}{|v|} \right]; \quad \gamma_{pl} = 2\gamma_0 \frac{\delta - 1}{\delta}. \quad (12)$$

This is a linear approximation to the friction force near to the two stable velocities $v = \pm v_0$.

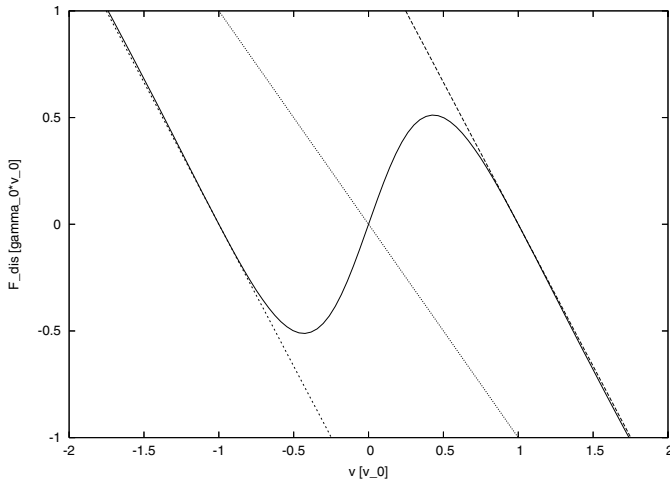


Fig. 1. Dissipative force for the parameter values $\delta = 0$ and $\delta = 2$ and a piecewise linear approximation for $\delta = 2$.

The units can be chosen that $m = 1$, $\sigma = 1$ and $\omega_0 = 1$. Further, in the numerical part, we will take the special values $v_d = 1$, $\gamma_0 = 1$. Choosing these *c.u.*, equation (4) becomes

$$\frac{d}{dt}v_i + \frac{\partial U}{\partial x_i} = \left[\frac{\delta}{1 + v_i^2} - 1 \right] v_i + \sqrt{2D} \xi_i(t).$$

3 Equilibrium configurations and attractors of the dynamical system

In the limiting case of constant friction $\gamma_0 > 0$, no driving $\gamma_1 = 0$ and no noise $D = 0$, the system will lose in the course of time its kinetic energy and go to the minima of the potential energy. Hence it will take certain equilibrium configurations. Morse rings have a potential landscape showing many minima [8–11, 19]. This allows a rich variety of clustering phenomena, due to the attractive forces between n.n. at distances beyond the potential minimum. The character of the equilibrium configurations of the particles on the ring essentially depends on the mean particle density $n := N/L$. Instead of n we may also consider the mean length (mean distance between the particles) $l := 1/n = L/N$. The effects of density variation at low temperatures may be studied by investigating the total potential energy $U(x_1, \dots, x_N)$. A particle configuration is a *stable state* of the ring, if it corresponds to a local minimum of U . Noteworthy is that in a ring with Toda interactions, for arbitrary values of n , only one stable state exists, given by the equidistant configuration [5]. At high densities

$$n > \frac{b}{\ln 2 + b} =: n_c. \quad (13)$$

Morse rings are completely equivalent to Toda rings, since the exponential repulsion dominates since for always corresponding to a minimum of U . For big densities, Morse rings with the parameter b behave like Toda rings with

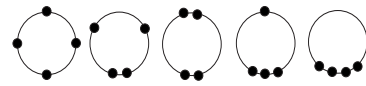


Fig. 2. Schematic representation of the Morse ring with $N = 4$ particles. The equidistant configuration (left) corresponds to a minimum of the Morse potential at high density, $n > n_c$, the single big cluster (right) is the only stable state if the density is low. In certain interval both equidistant and cluster configurations are stable states. The 3 central configurations correspond to saddle-points of U .

the parameter $2b$. On the other hand, in Morse rings with small density $n < n_c$, there may exist different types of stable states [9, 10]. Then, the equidistant configuration becomes a maximum of U and, therefore, it is unstable. However, for Morse rings there still exists a *second critical* value $\bar{n}_c(N) \geq n_c$, such that for $n < \bar{n}_c(N)$ new minima of U can be observed. These new stable states can be identified as the N equivalent configurations each corresponding to a single cluster of size N (see Fig. 2; extreme right configuration), which we refer to as ‘ N -mer’ in the following. For $N \geq 3$ there exists a transition interval (n_c, \bar{n}_c) , where *both* the N -mers and the equidistant configuration represent stable states; put differently, there is a coexistence region for qualitatively very different stable states [10]. In the remaining *low density* region $n < n_c$ the N -mers are the only stable configurations, and one can evaluate $Z_N^s = 2^N - 2 - N$ as the lower boundary for the number of saddle points in the $(N - 1)$ -dimensional potential energy landscape U . These meta-stable points correspond to symmetric combinations of smaller clusters (‘ k -mers’ with $1 \leq k < N$), as illustrated for $N = 4$ in Figure 2. Let us study now the case of driven systems and find their corresponding attractors. If the driving strength is weak enough i.e. $\delta < 1$, as in the passive case, the attractors are simply the minima of the global potential energy. For larger values $\delta > 1$, we observe *negative* friction at small velocities, then slow motions tend to be amplified. Therefore we find new attractors of motion, which are connected with the stable particle velocities $v = \pm v_0$. The general attractor structure might be very complicated and is known only for particular cases [11]. If the particle density is much larger than the critical density we may approximate the interaction by the simpler exponential potential. In this case the strongly driven system has (at least) $N + 1$ attractors [5, 11]. Hence, for $N = 4$ we should find at least 5 attractors of motion. The attractors are characterized by different values of the mean velocity V and the corresponding mean angular momentum M of the ring [5, 11]

$$V = \frac{1}{N} \sum_i v_i; \quad M = m \sum_i R_0 v_i. \quad (14)$$

Here R_0 is the radius of the ring. A rough estimate is based on a simple counting how many particles move in average to left or to right [5]. The combination of $N - k$ particles moving clockwise ($v_i > 0$) and k particles moving

counterclockwise $v_i < 0$ gives the estimate

$$V = \frac{N - 2k}{N} v_0; \quad M = mR_0(N - 2k)v_0, \quad (15)$$

where $k \leq N/2$. All the attractors provided by our estimate follow from a pitchfork-type bifurcation of the one (passive case) attractor at $\delta = 1$. For Morse rings, a complete analysis is known so far only for the case $N = 2$ [11].

4 Thermodynamic functions of the noninteracting system

In order to formulate a thermodynamics we need to define quantities like energy, entropy and temperature. Let us discuss this in general terms, for a system of N particles moving on a ring of length L . There exist different ways to define a temperature. There is the *bath* temperature (noise temperature) which, according to the Einstein relation, is

$$T_b = \frac{D}{k_B m \gamma_0}. \quad (16)$$

In our c.u. we get $T_b = D$. Then, we may define a *kinetic* temperature by means of the average kinetic energy, i.e.,

$$T_k = \frac{m \langle v^2 \rangle}{k_B}. \quad (17)$$

Third, we may introduce (in non-equilibrium) the *hydrodynamic* temperature which considers only the stochastic part of the kinetic energy,

$$T_h = \frac{m \langle (v - \langle v \rangle)^2 \rangle}{k_B}. \quad (18)$$

Finally, we may define the *entropic* temperature by means of the standard thermodynamic relation

$$\frac{1}{T_s} = \left(\frac{\partial S}{\partial E} \right)_V. \quad (19)$$

Although in equilibrium all these definitions coincide, in nonequilibrium they may lead to different values under the same conditions. Let us see this first for the simple case of noninteracting (free) particles.

For the case of free particles the stationary distribution functions, which are the solutions of the Fokker-Planck equation corresponding to the Langevin equation are known [22, 23]:

$$f(v) = C \exp \left[-\frac{v^2}{2D} + \frac{\delta v_1^2}{2D} \ln \left(1 + \frac{v^2}{v_1^2} \right) \right]. \quad (20)$$

The energy has only a kinetic contribution

$$E_{id} = N \int \frac{dx dv}{h} \frac{v^2}{2} f(v). \quad (21)$$

The entropy follows from

$$S_{id} = -k_B \int \frac{dx dv}{h} f(v) \cdot \ln f(v), \quad (22)$$

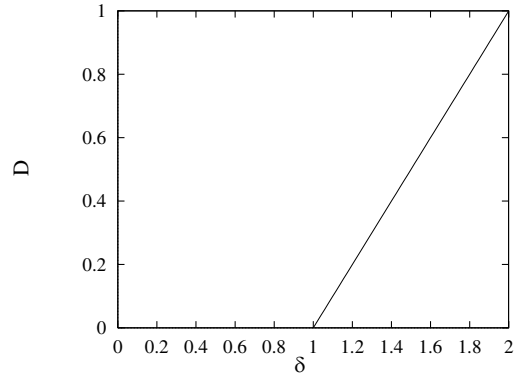


Fig. 3. Two different regions of noise strength and driving force: In the left near-equilibrium region the noise dominates, we have approximately equilibrium conditions. The thermodynamic equilibrium itself corresponds to the axis $\delta = 0$. In the right far-equilibrium region, the dynamical system has several deterministic attractors. The corresponding probability distribution may have several maxima around the location of the deterministic attractors.

where h is Planck's constant. In the case of thermodynamic equilibrium, the Maxwell distribution holds, and all temperatures are equal to the noise temperature $T_b = T_k = T_h = T_s = T = D$. For energy and entropy we get in dimensionless units

$$E_{id0} = \frac{N}{2} T \quad (23a)$$

$$S_{id0} = N \left(\frac{1}{2} \ln T - \ln n \right) + \text{const.} \quad (23b)$$

In nonequilibrium we cannot solve the integrals explicitly, but we have only one-dimensional integrals which are easy to treat numerically. In the calculations we have to distinguish between the two regions shown in Figure 3. In the left/upper region the noise dominates, i.e. approximately equilibrium conditions with Maxwell distributions

$$f(v) = \text{const.} \times \exp \left[-\frac{v^2}{2D} \right]. \quad (24)$$

Energy and entropy are given by the equilibrium expressions with the noise temperature instead of the thermodynamic temperature:

$$E_{id1} = \frac{ND}{2} \quad (25a)$$

$$S_{id1} = N \left(\frac{1}{2} \ln D - \ln n \right) + \text{const.} \quad (25b)$$

In the right/lower region the velocities are bistable, always near to one of the deterministic attractors $v = \pm v_0$, the dispersion (mean square deviation from these characteristic velocities) is small. Assuming a piecewise linear friction law (Fig. 1) the distribution may be approximated by

$$f(v) = \text{const.} \times \exp \left[-\frac{\gamma_{pl} (|v| - v_0)^2}{2D} \right]. \quad (26)$$

This is a symmetrical bistable distribution corresponding to the two most probable values of the velocity. The effective dispersion around the most probable values of the velocity is determined by

$$D^* = \frac{\gamma_{pl}}{D} = \frac{D\delta}{2(\delta-1)}. \quad (27)$$

Energy and entropy as above come from the two (positive/negative) branches of the distribution

$$E_{id2} = \frac{N}{2}(v_0^2 + D^*). \quad (28)$$

Here the first contribution corresponds to the stable velocity and the second one is determined by the dispersion around it. The entropy is given by

$$S_{id2} = N \left(\frac{1}{2} \ln D^* - \ln n \right) + \dots \quad (29)$$

Thus for the region of bistability the ideal entropy contribution:

$$S_{id2} = N \left(\frac{1}{2} \ln D - \ln n + \ln \left(\frac{\delta}{\delta-1} \right) \right) + \dots \quad (30)$$

In order to calculate the ideal pressure we assume that the ideal pressure is the momentum exchange of the stochastic motion with the wall. This gives for regions 1 and 2 respectively:

$$p_{id1} = n \langle v^2 \rangle = nD, \quad (31)$$

$$p_{id2} = n \langle v^2 \rangle = n(v_0^2 + D^*). \quad (32)$$

Let us now calculate the contributions due to the Morse interactions of the particles by computer modelling.

5 Numerical calculations of the interaction contributions

We calculated the interaction contributions to the energy, e_{in} , the pressure, p_{in} , and the entropy, S_{in} , which are due to the forces between the particles. These quantities are estimated by processing the data about the trajectories of the particles extracted from computer experiments, using suitable algorithms. Before we proceed to discuss the results of the numerical modelling, it seems useful to further clarify the meaning of the interaction parts e_{in} , p_{in} and S_{in} , taking into account the possible clustering of particles in the Morse chains.

First we will describe the thermodynamic functions for *passive* particles and, subsequently, will proceed to consider the characteristic features of *active* interacting particles. The interaction contributes the potential energies U_i of all pairs of particles to the total energy

$$e_{in} = u = \lim_{\tau \rightarrow \infty} \frac{1}{\tau} \int_0^\tau \frac{1}{N} \sum_{i=1}^N U_i dt. \quad (33)$$

A time average is carried out instead of an ensemble average assuming ergodicity of the system of passive particles. The contribution of the interaction to the pressure is calculated as a time average using the virial theorem

$$p_{in} = n \left\langle \sum_{i=1}^N \frac{\partial U_{ji}}{\partial r_{ji}} r_{ji} \right\rangle. \quad (34)$$

The contribution of the interactions to the entropy was only roughly estimated taking into account the possible clustering of particles and the directions of motion. We construct a rudimentary phase space in which only the composition of clusters in the chain and the directions of motion of clusters (to the right/ or to the left) distinguish the states of the system. For example, the ensemble of $N = 4$ particles forming two dimers possesses four states, the most ordered configuration – one big cluster (N-mer) – is the only state for the *passive* regime ($0 < \delta < 1$) with a zero mean velocity ($\delta < 1$) and two others for the *active* regime ($\delta > 1$) with the two stable velocities; the least ordered configuration – the gas-like regime – has 16 states. Because of the small number of configuration states in ensembles of a small number of particles, the sought quantity

$$S_{in} = \ln \Omega + \text{const.} \quad (35)$$

may be calculated directly from trajectories of particles by using an algorithm developed by Ma [25]. Here Ω is the number of micro-states of the system with the constant chosen to satisfy the condition $S_{in} \rightarrow 0$ in the gas-like state at high temperature. Certainly, the estimate of S_{in} (it may be called the “configuration entropy”) is approximate but it gives, as we will show below, reasonable results in both cases, for *passive* and *active* particles as well. Of course we are aware that the entropy for non-equilibrium states is an ill – defined concept. Noteworthy is an alternative method to calculate the entropy evolution of microscopically simulated far-from-equilibrium structures [26].

The numerical integration of the stochastic Langevin equation (8) was performed by using a fourth-order Runge-Kutta algorithm, especially adapted for solving stochastic problems [10,27]. In all computer experiments the heat bath is realized by Gaussian random numbers. Moreover, we always start with equal distances between the passive particles, $r_i = 1/n$, and all particles initially at rest, $v_i(0) = 0$. We may assume that the stationary state of the heated passive ensemble does not depend on initial conditions. At variance to this simple situation, the ensemble of *active* particles has several attractors [8,9] with corresponding basins. At low temperatures the ensemble occupies one of the attractors getting there from a chosen initial state and staying there. In this case each of the quantities, defined above, may take different values, depending on which of the attractors is occupied by the system. In principle, it is possible to calculate the probability of realization of any state, estimating a relative phase volume of the corresponding basin of attraction. It allows to introduce the averaged values for e_{in} , p_{in} , and S_{in} . However, the physical meaning of the values defined in such

way is far from clear. Moreover, a numerical averaging over all possible stochastic transitions between the attractor basins takes a very long computer time, in particular at low noise strength. For these reasons we will study here (at low values of noise strength) only the most typical stationary states and study their transitions with increasing temperature. In our computer experiments the integration step is fixed to $dt = 0.001$ or $dt = 0.00125$ (in *c.u.*). Each run consists of two stages: First the ring chain is heated to the temperature corresponding to the given bath temperature D ; at the second stationary stage, i.e., when the time averages of characteristic physical quantities do not change anymore, measurements are made by recording long trajectories. We restrict ourselves to the study of the processes occurring in low-density rings ($n < n_c$) focusing on details of the clustering phenomena in ensembles of both *passive* and *active* particles as. All results in this section refer to ensembles with densities in the range $n = 1/3 < n_c = 0.59$. (This density region corresponds to parameter values with no multi-stable states. We come back to this point in Section 7, observing the cluster phase diagrams.) We consider ensembles for three typical values of the bifurcation parameter $\delta = 0.0, 2.0, 1.2$. The first of them corresponds to the *passive* regime (Fig. 3), the second refers to the *active* regime with dominance of deterministic factors in the wide region of the temperature D . The third parameter set ($\delta = 1.2$) corresponds to the transition region, where *active* behavior is observed only at low values of the temperature D .

5.1 Passive particles $\delta = 0$

Let us first study the simplest case of rings of *passive* particles corresponding to thermodynamic equilibrium. The dependence of the average potential energy $e_{in} = u = \langle U \rangle$ (Fig. 4) on the temperature D looks as expected. At low temperatures we find the potential energy $u \simeq u_{min} \simeq (-0.5 \times 3)/4 = -0.375$ corresponding to the state where four particles form a single 4-cluster with equilibrium distances $l \simeq 1$. On the other hand, the interaction energy tends to zero when the temperature increases. In fact, u does not reach the zero value in the considered $D \leq 1$ temperature range but the tendency is clear. The region of the fastest growth of e_{in} corresponds to the “liquid-like state” of the ensemble [10] (recall the results of Sect. 6). Note that for non-equilibrium states, $\delta = 1.2$ and 2.0 , the dependence on the noise temperature D is much more complicated. We observe the energy corresponding to the highest ordered cluster state only in certain window of the noise strength. The curves for the interaction part of the entropy S_{in} vs. D (Fig. 4b) correspond to the $u(D)$ dependence. The interaction contribution to the entropy increases from the value $S_{in}^{min} \simeq -2.8$, corresponding to the minimal configuration entropy (in our definition), at low temperatures, and it vanishes in the gas-like state. Besides, it changes from the minimum to the maximum in the same temperature range as observed for $u(D)$. In the same temperature range a typical behavior of the interaction contribution to the pressure $P_{in}(D)$ is observed

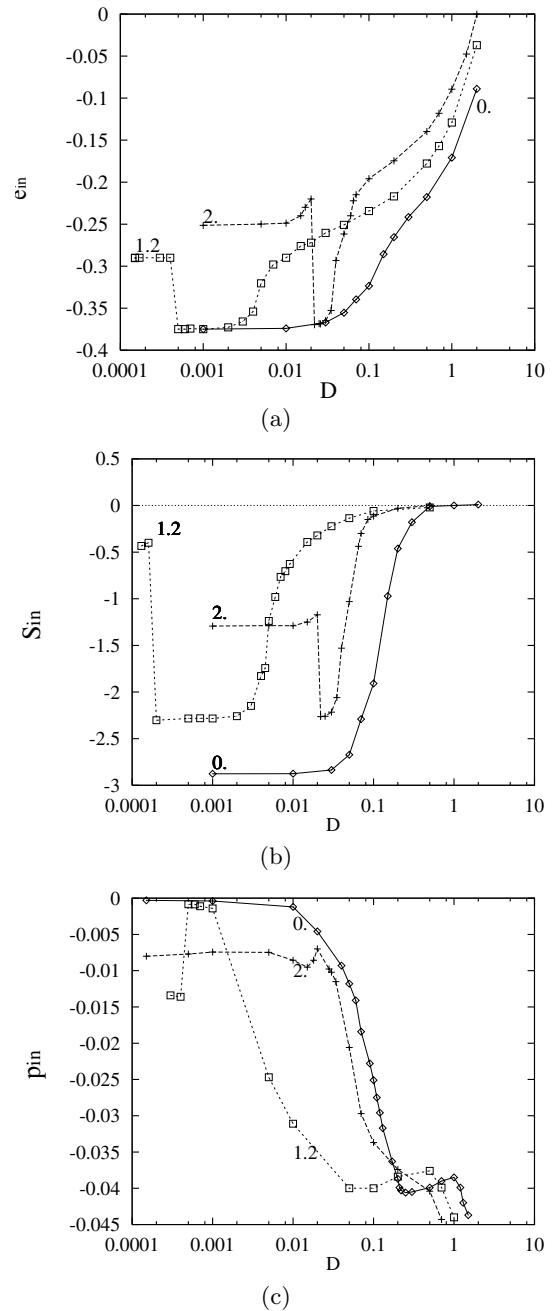


Fig. 4. Morse ring with $N = 4$, $b = 1$ and l . Numerically calculated contributions of the interaction effects to the thermodynamic potentials as a function of the temperature (noise strength D): (a) internal energy, (b) entropy, (c) pressure. The specific volume is fixed at $l = 1/n = 3$. The case of equilibrium $\delta = 0$ is compared with the cases of “near critical” non-equilibrium $\delta = 1.2$ and strong non-equilibrium $\delta = 2$.

(see Fig. 4c). The “interaction” part of the pressure is negative and very small at low temperatures (Fig. 4c) corresponding to the formation of only one big cluster with free ends. But with increasing noise the cluster is destroyed, p_{in} falls rapidly, corresponding to a transition “crystal-liquid”. In the following region ($0.2 < D < 1.0$) the pressure contribution is again approximately constant

corresponding to a “liquid-like state”. Finally it follows a noise region ($D > 1$), where the pressure contribution falls down with increasing noise temperature, corresponding to a “gas-like-state”.

5.2 Active particles far from equilibrium $\delta = 2$

At low temperatures the particles move regularly on the ring, only weakly disturbed by the noise of the surrounding bath. Hence the finite value of $u(D)$ at $D \rightarrow 0$ reflects the contribution of several dynamical excitations (nonlinear oscillations such as solitons, etc. [19]). Three kinds of regular motion are observed in the 4-particles ensemble, according to the initial state of the system:

- a) One big cluster is running as a whole, clockwise or counterclockwise. We will call this the state St_1 with the probability for clusters $P_D(k) = (0, 0, 0, 1)$, where $k = 1, 2, 3, 4$ is the expected number of particles in the cluster [9],
- b) Pairs of particles (dimers) are formed which show so-called “optical” oscillations, because the dimers oscillate in anti-phase. We call this state St_2 with $P_D(k) = (0, x, 0, 1 - x)$, $0 < x < 1$,
- c) Two oscillating non identical clusters – a mono-mer and a three-mer – are formed. These clusters are superimposed on the collective rotation of this group of two clusters (on the right/left). This state is called St_3 with $P_D(k) = (y, 0, y, 1 - 2y)$, $0 < y < 0.5$. Both values x and y depend on the specific volume l and, for instance, $x = 0.66$ and $y = 0.33$ for the considered ensemble with $l = 3$. They increase when l increases.

The states St_2 and St_3 have about the same values for the configuration entropy S_{in} but a different relationship between of the temperatures introduced above – $T_k = T_h$ for St_2 and $T_k > T_h$ for St_3 . The behavior of the ensemble in the state St_2 is reduced to that in the 2-particle ensemble studied in detail in [9]. It is worth recalling results from the earlier study of the dynamics of the St_3 -state of the ensemble because it also corresponds to the interaction of two “particles” though not identical. If we denote the configurations in Figure 2 in accordance with their cluster composition (from the left to the right) as $(1 + 1 + 1 + 1)$, $(2 + 1 + 1)$, $(2 + 2)$, $(3 + 1)$ and $(4 + 0)$, one can interpret the state St_2 as transitions from the configuration topologically like $(4 + 0)$ to one topologically like $(2 + 2)$ and back. Similarly, the state St_3 is the transition between a configuration like $(4 + 0)$ and one like $(3 + 1)$. Another possible state obtained with participation of other, more complex, structures $2 + 1 + 1$ and $1 + 1 + 1 + 1$, has been found to be unstable. They are born sometimes during the transition process but always decay (at least, in all of our computer simulations) into one of the other mentioned above.

Before we begin to illustrate the results of the numerical estimations for the thermodynamic quantities, let us discuss the probability of excitation of any kind of regular states of the ensemble. For that the simulation was performed placing the particles at the initial time at rest and at equal distances, r_0 . Varying the distance r_0 from $r_0 = 1$ up to $r_0 = l$, one can control the initial value of

the energy into the ensemble, $e_0 = u_0$. Besides, the quantity $\Delta u = u_0 - u_{min}$ may serve as a bifurcation parameter defining the initial ability of the system to be in a non-equilibrium state. Varying Δu from 0 at $r_0 = 1$ up to 0.25 at $r_0 = l = 3$. and changing the initial state of the noise generator we found that if $0 < \Delta u < 0.0001$, only the state St_1 is excited; if $0.0001 < \Delta u < 0.001$, the state St_1 or St_3 can be excited depending on the initial state of the noise generator, and besides, the state St_1 prevails near the lower boundary of the range and St_3 near the upper one; if $0.001 < \Delta u < 0.0015$, only the state St_3 occurs; at $0.0015 < \Delta u < 0.007$, the states St_3 or St_2 are established; at $0.007 < \Delta u < 0.2$ there is only the state St_2 ; and finally if $0.2 < \Delta u < 0.25$, both states St_3 and St_2 can be excited again. Thus, the ensemble settles at the state St_1 only for very particular conditions, when the initial state corresponds to a very low energy. But if the bifurcation parameter δ exceeds the rather small value $\delta_1 \simeq 0.0001$ this state loses stability and the oscillatory mode takes over. Most frequently we observe the “optical” oscillations of pairs of dimers accompanied by rotations of the ensemble as a whole with superimposed regular oscillations of two dimers moving towards each other. In our simulations we have never seen the steady-state regime in which the ensemble transfers from the state St_2 to the one St_3 and back, although this state is possible.

The potential energy and the configuration entropy do not appreciably change ($e_{in} \approx \text{const.}$ and $S_{in} \approx \text{const.}$) in this temperature range $D \leq 0.01$ but, of course, both $u > u_{min}$ and $S_{in} > S_{inmin}$ (Figs. 4a and 4b). The initial conditions are chosen as described above, with $r_0 = l$. With increasing D there is the striking effect that the increasing noise of the surrounding bath stimulates the system to pass to the most ordered state with only the big N-cluster, characterized for the active ensemble by the minimal values of both u and S_{in} . The transition to the single-cluster state happens at $D \approx 0.02$, and only at $D \geq 0.04$ the cluster begins to decay and the potential energy and configuration entropy grow in agreement with each other. Note, however, that the state St_2 – “optical” oscillations of the pair of dimers – is more stable than the St_3 and transforms to the state “one-big-cluster” in a much more limited parameter range of the increasing temperature D relative to the state St_3 . However, this follows only from a limited number of runs for the state St_2 .

Returning to the results for the state St_3 we find that the curve p_{in} (Fig. 4c) is shifted to lower temperatures also, but the pressure range corresponding to “one-big-cluster state”, is very narrow. The range of regular behavior occurs at very low D . However, strictly speaking, at $D \rightarrow 0$ thermodynamic functions make no sense since the dynamical system is multi-stable and has several attractor regions. In principle for any finite value of the noise the separatrices between the attractors are transparent but transitions may be very rare. For this reason very long trajectories are required and we run into numerical difficulties. At high values of the noise all curves tend to the results for thermodynamic equilibrium.

5.3 Active particles near to the border of excitation $\delta = 1.2$

The ring with $\delta = 1.2$ is chosen in order to study the transition phenomena between the two regions shown in Figure 3. In the parameter space (δ, D) (Fig. 3) this system is placed near the boundary between the two earlier mentioned regions with different relation of noise strength and driving force at low temperature. For these systems we observe the lowest temperature D_{23} of transition to the “gas-like state” [10] (that is the transition from the region 2 to the region 3 in Figure 7a, see also Sections 6 and 7 below). Since for $D \simeq 0.1$ this system is rather near to the boundary between two regions in the parameter space (δ, D) (Fig. 3), it is difficult to distinguish the peaks in the distribution near $v = \pm v_0$. However the numerical results presented in Figures 4a–c appear acceptable since they lay just between the cases $\delta = 0$ and $\delta = 2$. For example, the estimates for the entropy, look reasonable because the dependence $S_{in}(D)$ correlates with the dependence $e_{in}(D)$ and is similar to that observed for the ring with $\delta = 2$. Note, however, that the temperatures at which the system is in the most ordered state are much lower for the studied ring in comparison with the case of strong driving force ($\delta = 2$) where the corresponding temperature range is narrower. We will discuss the reasons for the observed effects in more detail in Sections 6 and 7, but before that let us consider the total thermodynamic functions, i.e. the sum of the ideal and the interaction contribution, in cases where we are able to do this.

6 Discussion of the total thermodynamic functions

In the parameter ranges where we calculated the ideal and the interaction contributions we can determine the total thermodynamic functions $e = e_{id} + e_{in}$, $S = S_{id} + S_{in}$ and $p = p_{id} + p_{in}$. We will analyze them in two cases – for the *passive* particles ($\delta = 0$) and for *active* particles with a rather big value of the deterministic velocity v_0 ($\delta = 2$), both systems corresponding to regimes far from the boundary dividing the regions left/upper and right/lower in Figure 3. The more difficult case of the transition region between the two regimes is not considered here.

6.1 Equilibrium regime $\delta = 0$

For the ring of *passive* particles the thermodynamic characteristics look like the classical ones; the energy and entropy grow with increasing temperature D in accordance with the temperature behavior of kinetic and potential energies (Fig. 5). The kinetic energy $T_{kin} = 2 \cdot T_k(D)$ is shown in the Figure 5a together with the energy $e(D)$, and with $T_k \approx T_h$ in this case.

To analyze the changes in the pressure due to variation of parameters, isotherms p versus specific volume $l = 1/n$ at $D = \text{const.}$ are plotted (see Fig. 5c). We represented

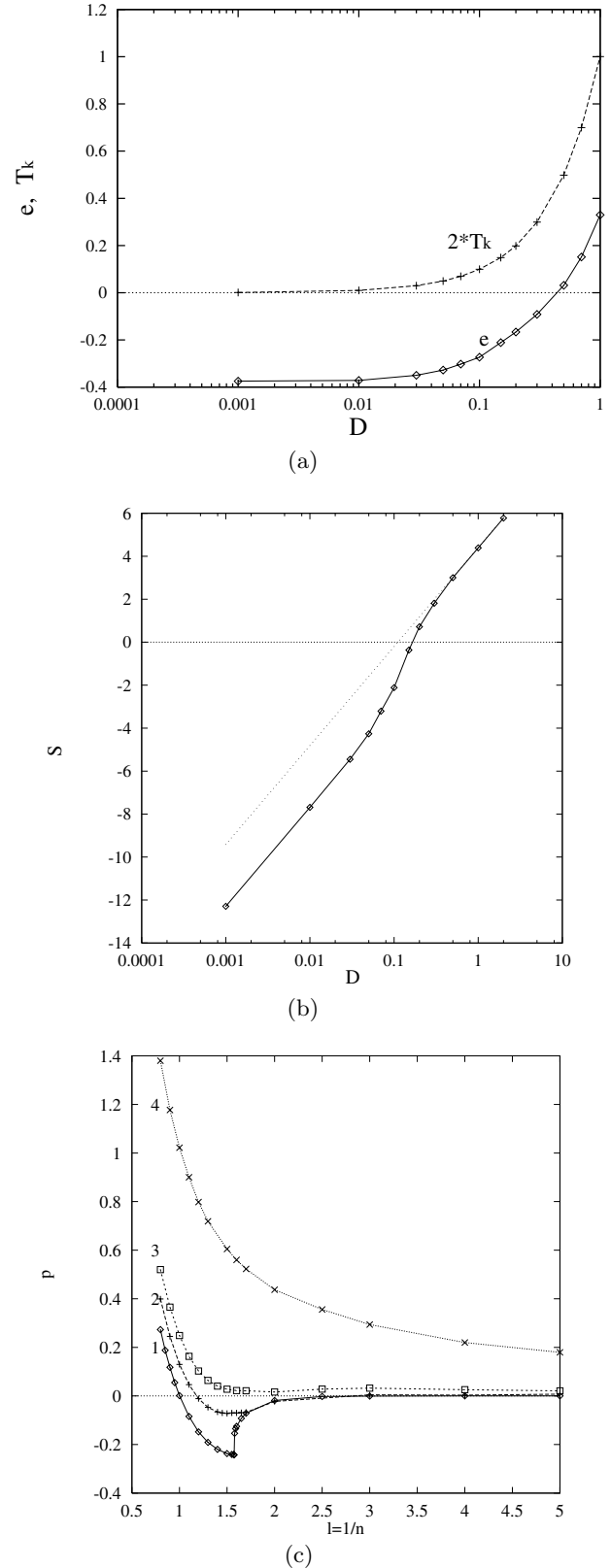


Fig. 5. Morse ring with $N = 4$, $b = 1$ and *passive* friction $\delta = 0$. (a) Energy e and kinetic energies $2 \cdot T_k$ and (b) entropy S vs. temperature D for specific volume $l = 1/n = 3$, and (c) isotherms P vs. specific volume $l = 1/n$ at $D = \text{const.}$ Curves at (c) for: 1- $D = 0.001$, 2- $D = 0.01$, 3- $D = 0.1$, 4- $D = 1$.

the isotherms for a wide range of density values, both for $n > n_c$ and $n < n_c$, to illustrate the anomalous behavior of the isotherms at small D near the critical density n_c , as earlier observed [10]. The new results support the conclusion about the specific change with density in the pressure near n_c caused by transitions between multi-stable states when $n \approx n_c$ and $D \ll \epsilon = 0.5$ (here ϵ is the depth of the Morse potential defined above). The virial method for the determination of the pressure which we use here, allows to describe correctly the behaviour of the pressure; it is negative in the regime of one stable big cluster with free ends. This improves the method of average force used in [10], which does not distinguish attractive and repulsive forces.

6.2 Far-equilibrium regime $\delta = 2$

Before analyzing the standard thermodynamics characteristics let us consider the behavior of the temperatures T_k and T_h in Figure 6a. One can see that they clearly differ at low temperature when the particles do not move chaotically. Hence, the system moves as whole in the state St_3 and particles oscillate in the ring. But if the ensemble passes to the big-cluster state then T_h goes to zero. The energy e also falls in spite of T_k increasing; the ring begins to rotate faster. Thus, the increasing noise drives the ensemble to a more ordered state. Only if the noise intensity exceeds some level, e , T_h and then T_k begin to grow. The entropy (see Fig. 6b) behaves with changing D in full accordance with e , T_k and T_h . We observe that S decreases when D grows, and if one did not know that the system is open, the phenomenon could be surprising. It should be noted that such a behavior is reminiscent of effects found in stochastic and chaotic resonance [28,29]. Indeed finite noise may have an ordering influence in many cases. However, we shall not dwell on this question here.

Finishing the analysis of thermodynamic characteristics by considering the pressure dependence on density (Fig. 6c) we may conclude that the most interesting features of the pressure behavior are connected with having multi-stable states near the critical density as in *passive* rings. One can observe an anomalous change of pressure values with density, only at lower temperatures relative to the *passive* ring. As we limit ourselves to the study of effects of clustering in this work, we leave the problems connected with multi-stable states for a future study.

7 Phases in equilibrium and non-equilibrium

In addition to the above mentioned physical quantities, we also consider the probability of cluster configurations $P_D(k)$ to identify the phase state of the ensemble studied. In accordance with earlier work [9], the cluster distribution $P_D(k)$ is defined as the probability for finding a cluster of size k in the ring at time $t \gg 0$ at the temperature D . Accordingly, for the one-big-cluster state $P_D(4) = 1$, $P_D(k < 4) = 0$, the gas-like state is that with $P_D(k) > P_D(k + 1)$. The other case is qualified as

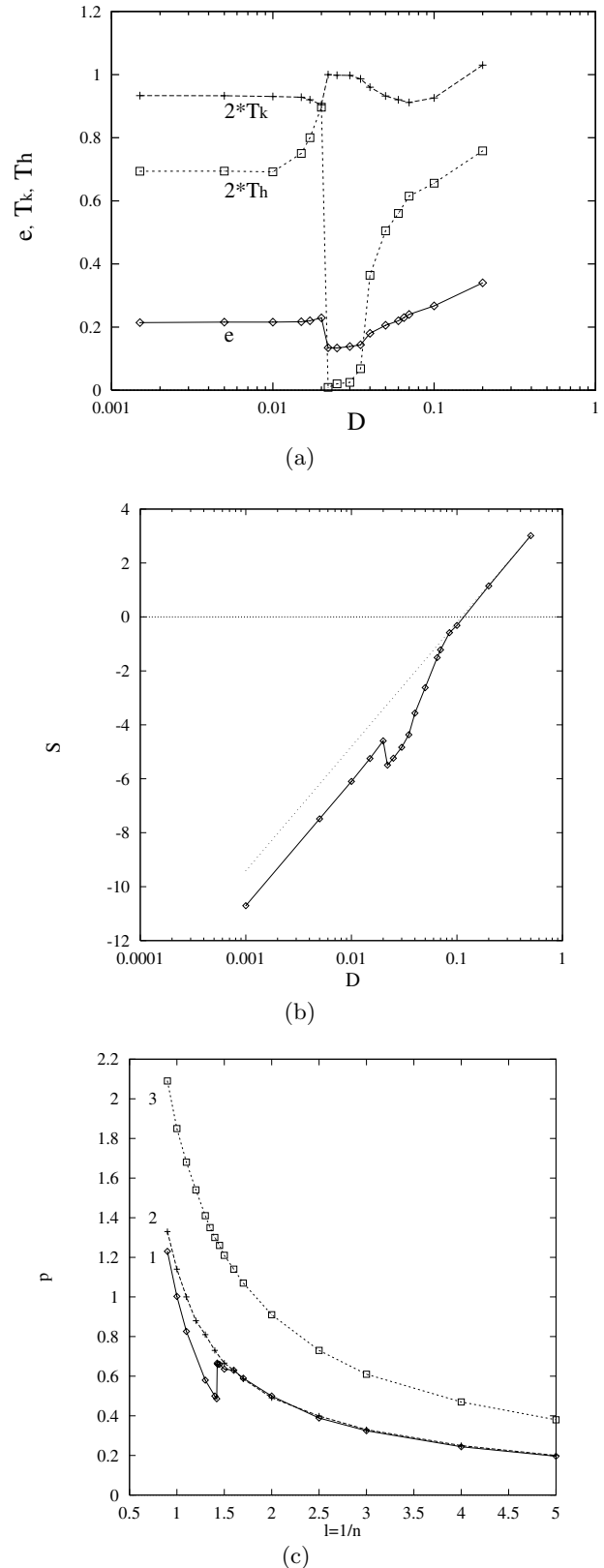


Fig. 6. Morse ring with $N = 4$, $b = 1$ and active friction $\delta = 2$. (a) Energy e and kinetic energies $2*T_k$, $2*T_h$ and (b) entropy S vs. temperature D for specific volume $l = 1/n = 3$, and (c) isotherms P vs. specific volume $l = 1/n$ at $D = \text{const}$. Curves in (c) for: 1- $D = 0.001$, 2- $D = 0.1$, 3- $D = 1$.

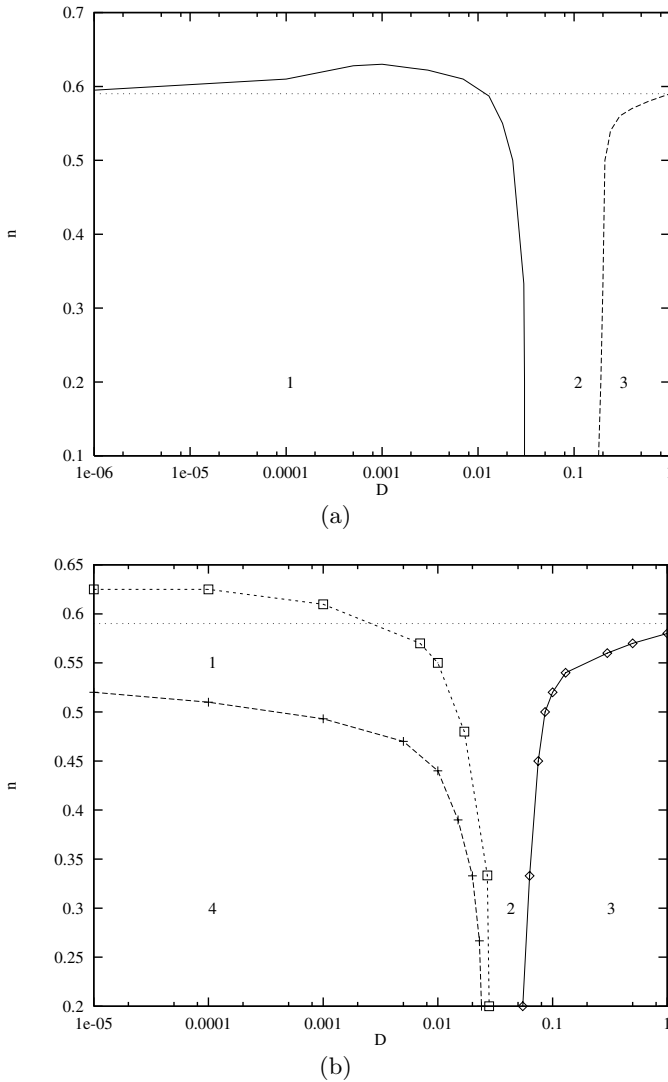


Fig. 7. Cluster phase diagram for the Morse ring with parameters $N = 4$, $b = 1$ with both (a) *passive* friction ($\delta = 0$.) and (b) *active* friction ($\delta = 2$.) The lines symbolize transitions between different phase states: 1 - one big cluster (N -mer), 2 - small clusters (“liquid-like phase”), 3 - monomers prevail (“gas-like phase”), 4 - multi-stable stationary states.

liquid-like state for *passive* particles, although it may characterize, besides, the regular modes at low temperatures in ensembles of *active* particles. In Figure 7a “phase diagram” of states identified using the numerically determined values for $P_D(k)$ is given for both a *passive* system ($\delta = 0$) and an *active* one ($\delta = 2$.) with the state St_3 at low temperature and sufficiently low enough density. The diagrams show regions with different states of an ensemble with $N = 4$ particles in the temperature D -density n -plane of a low-density ring ($n < n_c$). The diagram for the *passive* ensemble (see Fig. 6a and see also [10]) is divided in three parts by two boundary curves, $n(D_{12})$ and $n(D_{23})$ indicating the transitions between different states. The states are: one-big cluster (region “1”) at low temperatures, the gas-like one (region “3”) at high tem-

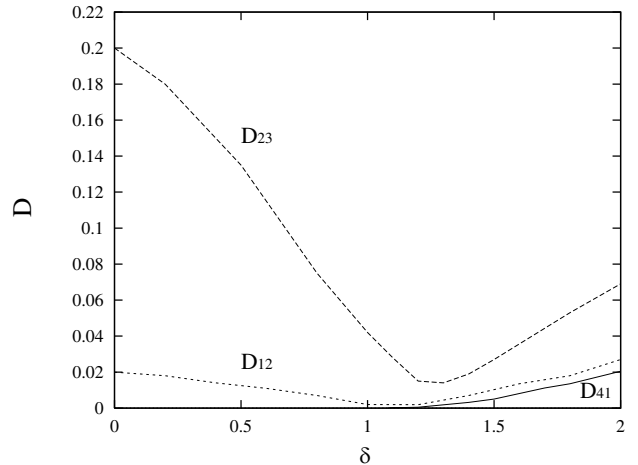


Fig. 8. Active Morse ring with $N = 4$, $b = 1$ and $l = 1/n = 3$. Noise amplitudes D_{12} , D_{23} and D_{41} corresponding to transitions between different phase states as functions of δ .

peratures and a liquid-like state (region “2”) at intermediate temperatures of order of the depth $\epsilon = 0.5$ (in c.u.) of the Morse potential well with $b = 1$. In the diagram also a part of the region “1” at $n > n_c$ is shown which represents the boundary $n(D_{12})$ [10].

What happens when the parameter δ is increasing from zero up? If $0 < \delta < 1$ the behavior is simply like that with a smaller friction coefficient $\gamma > 0$. The transition curves $n(D_{12})$ and $n(D_{23})$ are shifted to lower temperatures (Fig. 8) but the dynamics of particles does not change basically. But with increasing δ new states arise in the phase diagram left/lower (region 4) at the transition $\delta > 1$. These states are characterized by regular oscillations of particles on the ring or by nonlinear waves (rotational mode). In the range $0 < \delta < 1.2$ the transitions curves n_{12} , D_{12} and n_{23} , D_{23} fall down to a minimum of the temperature. However when $\delta > 1.2$ they increase again. The region “1” shrinks at low densities and at $\delta = 2$ the phase diagram looks as at Figure 7b. The one-big-cluster (“crystal-like state”) exists in the narrow range of density values near n_c and a very narrow temperature range at low density. It is possible that it vanishes with further increasing δ and then the system passes from the state “4” to the state “3”. Note, that the region “4” possesses a very complex structure because here we may have a number of stable stationary states, corresponding to different rotational and oscillatory modes. Strictly speaking, the usual thermodynamic concepts break down in region “4” at least near to $D \rightarrow 0$.

8 Summary and conclusions

In this work we have provided numerical results for a $1 - d$ model of 4 Brownian particles with both *passive* and *active* friction, interacting in a $1 - d$ box with periodic boundary conditions. We considered n.n. Morse interactions, which are repulsive at short distances and attracting at intermediate and long distances. Using this type of interaction our model tends to behave similar as a Lennard-Jones chain.

A Morse ring can be characterized by a critical density value n_c . For $n < n_c$ clustering states (k -mers) are basic states for the system. In combination with the possibility for *active* Brownian particles to get non-thermal energy from an external reservoir this leads to interesting effects, when the ring is coupled to a heat bath.

The stochastic Langevin equations of motion were numerically integrated using a suitable 4th order Runge-Kutta method. On the basis of the numerical solutions, thermodynamic quantities such as entropy, pressure and kinetic and potential energies were calculated. In addition, the distribution of clusters was estimated from the trajectories of particles. Also, phase diagrams for different density and temperature values were calculated for both *passive* and *active* particles. By analyzing the diagrams for a finite-size Morse ring ($N = 4$), three different thermodynamic states are found for a low density ensemble of *passive* particles and for the ensemble of *active* particles.

Due to external non-thermal pumping, the system may be driven to far-from-equilibrium states. The numerical results indicate that such an additional energy exchange mechanism can select configurations of particles in the ring at low temperature allowing in the ring only a few simple configurations. They are the one big cluster and anti-phase oscillations of two groups of particles (k -mers). States with “optical” oscillations prevail in the system, and only in a limited parametric range the noise of the bath may order the behavior of the system exhibiting properties akin to some kind of stochastic resonance.

A range of temperature exists in which the ensemble transforms from the regular state with negligible influence of the thermal bath to a weak ordered state like a gas. The range is shifted when changing the level of external pumping, and the lowest temperature of the transition is found to be at the value of the parameter of pumping little above the critical value. In conclusion we may state that the simple system studied here, gives some insight on how the concepts of phase state and phase transitions may be extended to nonequilibrium.

The authors thank Jörn Dunkel, Valeri Makarov and Jörn Schmelzer for help and for useful discussions.

References

1. M. Toda, *Nonlinear Waves and Solitons* (Kluwer, Dordrecht, 1983)
2. Stochastic Dynamics of Reacting Biomolecules, edited by W. Ebeling, L. Schimansky-Geier, Yu. Romanovsky (World Scientific, Singapore, 2002)
3. S.E. Trullinger, V.E. Zakharov, V.L. Pokrovsky, *Solitons*, edited by (North Holland, Amsterdam, 1986)
4. M. Janssen, W. Ebeling, *Physica D* **141**, 117 (2000)
5. W. Ebeling, U. Erdmann, J. Dunkel, M. Janssen, *J. Stat. Phys.* **101**, 443 (2000)
6. V. Makarov, W. Ebeling, M.G. Velarde, *Int. J. Bifurcation & Chaos* **10**, 1075 (2000)
7. W. Ebeling, A. Chetverikov, M. Janssen, *Ukrain J. Phys.* **45**, 479 (2000)
8. J. Dunkel, W. Ebeling, U. Erdmann, *Eur. Phys. J. B* **24**, 511 (2001)
9. J. Dunkel, W. Ebeling, U. Erdmann, V.A. Makarov, *Int. J. Bifurcation and Chaos* **12**, 2359 (2002)
10. A. Chetverikov, J. Dunkel, *Eur. Phys. J. B* **35**, 239 (2003)
11. V. Makarov, E. del Rio, W. Ebeling, M.G. Velarde, *Phys. Rev. E* **64**, 036601 (2001)
12. E. del Rio, V. Makarov, M.G. Velarde, W. Ebeling, *Phys. Rev. E* **67**, 056208 (2003)
13. F. Schweitzer, W. Ebeling, B. Tilch, *Phys. Rev. Lett.* **80**, 5044 (1998)
14. F. Schweitzer, W. Ebeling, B. Tilch, *Phys. Rev. E* **64**, 021110 (2001)
15. W. Ebeling, P. Landa, V. Ushakov, *Phys. Rev. E* **63**, 046601 (2000)
16. C.I. Christov, M.G. Velarde, *Physica D* **86**, 323 (1995)
17. V.I. Nekorkin, M.G. Velarde, *Synergetic Phenomena in Active Lattices. Patterns, Waves, Solitons, Chaos* (Springer, Berlin, 2002)
18. A.A. Nepomnyashchy, M.G. Velarde, P. Colinet, *Interfacial Phenomena and Convection* (Chapman & Hall, London, 2002)
19. E. del Rio, V.A. Makarov, M.G. Velarde, W. Ebeling, *Phys. Rev. E* **67**, 056208 (2003)
20. Yu.L. Klimontovich, *Statistical Physics* (Gordon & Breach, New York, 1986)
21. Yu.L. Klimontovich, *Physics-Uspekhi* **37**, 737 (1994)
22. Yu.L. Klimontovich, *Statistical Physics of Open Systems* (Kluwer, Dordrecht, 1995)
23. U. Erdmann, W. Ebeling, L. Schimansky-Geier, F. Schweitzer, *Eur. Phys. J. B* **15** 105 (2000)
24. J. Dunkel, W. Ebeling, J. Schmelzer, G. Röpke, *Physica D* **185**, 158 (2003)
25. Shang-keng Ma, *J. Stat. Phys.* **26**, 221 (1981)
26. H. Diebner, O.E. Rössler, *Chaos, Solitons & Fractals* **19**, 699 (2004)
27. N.N. Nikitin, V.D. Razevich, *J. Comput. Math. & Meth. Phys.* **18**, 108 (1978)
28. L. Gammaitoni, P. Hänggi, P. Jung, F. Marchesoni, *Rev. Mod. Phys.* **28**, 223 (1998)
29. V.S. Anishchenko, V.V. Astakhov, A.B. Neiman, T.E. Vadivasova, L. Schimansky-Geier, *Nonlinear Dynamics of Chaotic and Stochastic Systems* (Springer, Berlin, 2002)